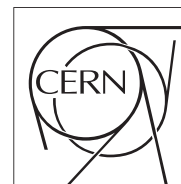


The Compact Muon Solenoid Experiment

# Detector Note

The content of this note is intended for CMS internal use and distribution only



2021/07/26

Archive Hash: 46865e6

Archive Date: 2020/06/30

Test Beam Study of SiPM-on-Tile Configu-  
rath<https://www.overleaf.com/project/5efe0d72121ad500013be9e6io>

## Abstract

Light yield and spatial uniformity for a large variety of CMS High-Granularity Calorimeter (HGCAL) prototype scintillator tiles was studied. The tiles are representative of tile shapes to be used in the scintillator section of the HGCAL. The light from each scintillator was collected by a Silicon Photomultiplier (SiPM) directly viewing the produced scintillation light (SiPM-on-tile technique). A range of tile sizes and a variety of scintillator base materials was studied. These studies were performed using 120 GeV protons at the Fermilab Test Beam Facility. External tracking allowed the position of each proton penetrating a tile to be measured.

This box is only visible in draft mode. Please make sure the values below make sense.

PDFAuthor: Michael Krohn  
PDFTitle: Test Beam Study of SiPM-on-Tile Configurations  
PDFSubject: CMS  
PDFKeywords: CMS, physics, your topics

Please also verify that the abstract does not use any user defined symbols



## 1 Introduction

The High Luminosity phase of the Large Hadron Collider (HL-LHC) [1] is scheduled to begin at CERN in 2027, with a designed instantaneous luminosity of  $5 \times 10^{34} \text{ cm}^{-2}\text{s}^{-1}$ . In order to operate in this environment, a new high granularity calorimeter (HGCAL) [2] will be installed in the endcap regions of the CMS detector. In front layers of the calorimeter, where the fluence is highest, the design uses silicon sensors as the active material. In deeper layers, the design uses plastic scintillator tiles, with the scintillation light readout by silicon photomultipliers (SiPMs).

To achieve the required performance, uniform light collection across the face of individual scintillator tiles is important. The SiPM-on-tile technology, where the SiPM is located in a dimple machined into the tile surface, has been studied for the Calorimeter for Linear Collider Experiment (CALICE) [3–5]. These studies reported that for 97% of the tile area the response is within 10% of the average response. Similar studies are needed for the tile designs that will be used in the HGCAL. Some adjustment of the HGCAL SiPM-on-tile design may be required to cover the full range of tiles in the calorimeter. CMS HGCAL will use scintillator tiles of approximately square shape varying in size from roughly  $2.3 \times 2.3 - 5.5 \times 5.5 \text{ cm}^2$ .

We describe the apparatus and analysis used to study the responses of different scintillator tile geometries and materials using the Fermilab Test Beam Facility (FTBF) [6] at the Fermi National Accelerator Laboratory. In this note, we present measurements for a range of geometries and a variety of scintillator base materials of cast and injection moulded tiles.

## 2 Description of HGCAL scintillator geometry

The final configuration of the HGCAL scintillators and their geometry within the detector will be finalized at a later date. The latest description of the geometry can be found in the HGCAL Technical Design Report [2].

## 3 Test beam and DAQ setup

The Fermilab test beam setup and the DAQ used to readout the silicon strip tracker stations and the SiPM is described in detail in Ref [7].

## 4 Cosmic test stand setup

To further explore some issues that came up during analysis of test beam data, we built a small cosmic ray telescope. This was used for several studies, including the effect of SiPM insertion to different depths into the dimple, studies of light yield vs hole size in the foil wrapper, and light yield vs surface roughness of the dimple. Results for these studies will be presented below. The cosmic telescope consisted of 2 small scintillators (top counter  $4 \times 4 \text{ cm}^2$ , and bottom counter  $2 \times 2 \text{ cm}^2$ ) separated by 15 cm. Each counter was coupled to a SiPM and each SiPM signal was amplified by a PORKA 10X amplifier, discriminated, and a coincidence of the two was formed. The coincidence counting rate was about one per minute. Sample scintillator configurations were placed between the two counters. The SiPM viewing the sample was fed through a PORKA 10X amplifier and then read out by a DRS4, triggered by the cosmic coincidence. To monitor SiPM gain in real time, an LED weakly optically coupled to the sample was pulsed at 1 Hz. The induced signal in the SiPM was also read out by the DRS4. The intensity of the LED was set to supply roughly four photoelectrons (PE) per event, with the photoelectrons very well separated from noise. This provided the ability to constantly monitor the PE

42 calibration of the SiPM. (We note that we found the PE calibration was very stable and it was  
43 not necessary to make corrections.) The temperature of the SiPM was monitored by a PT10K.  
44 The small temperature variations were not corrected for. The photograph in Fig 1 shows the  
45 setup.

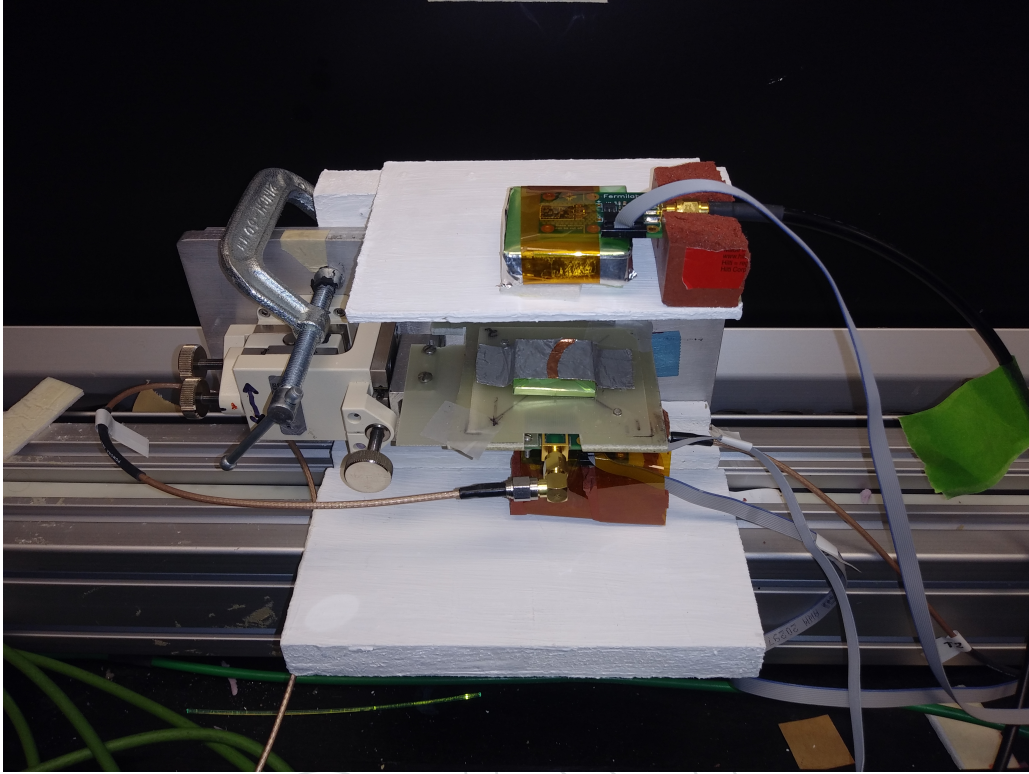


Figure 1: The cosmic ray telescope. A 4x4 cm scintillation counter is on top, and a 2x2 cm scintillation counter is on bottom. A sample scintillator (mounted on a green PCB) can be seen in the middle. The SiPM viewing the sample tile is independently mounted on an XYZ stage (cream colored in the photo). This permitted independent positioning of the SiPM relative to the tile, and was used, for example, in SiPM dimple depth studies.

## 46 5 Details of scintillator sample fabrication

47 This study's tile prototypes represent samples from small sets produced by different institu-  
48 tions in 2019/2020. Tiles EJ200, EJ208, and EJ262 were cut out of  $12 \times 12 \times .25$  inch sheets  
49 purchased by NIU from Elgen Technology. Tiles SC301 and SC307 were injection-molded by  
50 IHEP group (Protvino, Russia) and were also machined at NIU to their reported dimensions.  
51 Tiles IMn19, IMn21, IMn23, IMn24 were injection-molded at NIU (all sizes produced at the  
52 same time), and no follow-up machining was applied. No processing was applied to the tile  
53 prototype provided by the Kharkiv University group. Dimples in all tiles, except that from  
54 Kharkiv, were cut at the NIU facility.

## 55 6 Simulation

56 The expected optical responses of the various tiles were simulated using the GEANT4 [8]  
57 toolkit. The details of this simulation can be found in [7].



## 7 SiPM Calibration

A conversion factor between the integrated voltage and the number of the photoelectrons (PEs) produced in the SiPM was done following the procedure described in Ref [7].

## 8 Scintillator response

### 8.1 Event selection

We selected events which 1) have a matching trigger number for both DRS4 and tracker data, and 2) passed quality selection criteria. We required:

- a clean waveform - the falling edge of the signal pulse was required to reach the level of 0.25 of the pulse's maximum and the pre-signal region should be wider than the number of samples used for signal integration;
- noise suppression - SiPM signal pulses were required to have the peak amplitude above ten mV;
- clean tracker data - the upstream tracker station was required to have silicon strips fired in both x and y planes but have not more than one two-strip cluster in each.

These cuts were sufficient to ensure that a single particle passed through the tile and that the particle can be treated as a minimum-ionizing particle (MIP).

### 8.2 The light yield determination

To determine the light yield of a scintillator tile, the MIP yield distribution is fit with the sum of a Gaussian and a Landau function, where the lower light yield region is modelled to follow Gaussian statistics, but the high light yield tail is modelled with a Landau. We report the light yield as the most probable value (MPV) of the fit function. We observed that the MPV statistical uncertainty in a typical single measurement (5-10K clean events) was smaller than the  $\pm 3\%$  optical coupling systematic uncertainty described below in Ref [7].

### 8.3 Tile uniformity

To quantify a tile's uniformity, we divided a tile into  $2 \times 2$  mm<sup>2</sup> bins, determined the average light yield in each bin, and calculated the RMS/mean for all average light yield values in a given tile. To establish that the RMS/mean distribution provides useful insights on the uniformity of tiles, we performed a simplified simulation of a  $3 \times 3$  cm<sup>2</sup> tile. The simulated light response across the tile was perfectly uniform, following a Poisson distribution with an average light yield of 30 PE. We simulated 10 events in each  $2 \times 2$  mm<sup>2</sup> bin and compared the result to data by quantifying the non-uniformity as  $\frac{\text{RMS}/\text{mean}_{\text{tile}}}{\text{RMS}/\text{mean}_{\text{uniform}}} - 1$ .

## 9 Measurements

A summary of the measurements from the January and February test beams for a variety of tiles are grouped based on the SiPM used and its operating conditions in Tables 1, 2, and 3. In January, the Hamamatsu SiPM 13360-1350 operated at  $V_{op} = 54.5$  V was used. While in February, the Hamamatsu SiPM 13360-1350 operated at  $V_{op} = 54.25$  V and the Hamamatsu SiPM 14160-1315 operated at  $V_{op} = 41.83$  V were used. These tables contain the MPV, FWHM, and uniformity values for each tile.

96 To compare the light yield across a variety of scintillating materials, the MPV from all  $3 \times 3 \text{ cm}^2$   
 97 tiles is shown in Fig 2.

Table 1: Beam Test Jan 23-28 2020, 120 GeV protons, FTBF, Hamamatsu SiPM 13360-1350,  $1.3 \times 1.3 \text{ mm}^2$ ,  $V_{op} = 54.5 \text{ V}$ .

Runs	Tile Vendor	Wrapping	Area, mm $\times$ mm	MPV, PE	FWHM, PE	Non-Uniformity
Cast tiles, 3 mm thick						
690	Cast31x31, Kharkov, UA	ESR	31.0 $\times$ 31.0	35.8 $\pm$ 1.1	18.3	0.33 $\pm$ 0.07
651-8	EJ208, Texas, US	ESR	30.0 $\times$ 30.0	34.8 $\pm$ 1.0	18.0	0.23 $\pm$ 0.05
666-8	EJ200, Texas, US	ESR	30.0 $\times$ 30.0	33.9 $\pm$ 1.0	17.3	0.39 $\pm$ 0.05
758	EJ262, Texas, US	ESR	30.0 $\times$ 30.0	33.0 $\pm$ 1.0	16.5	0.42 $\pm$ 0.06
672-4	EJ200, Texas, US	ESR	34.0 $\times$ 34.0	25.8 $\pm$ 0.8	14.8	0.61 $\pm$ 0.05
688	EJ200, Texas, US	ESR	23.0 $\times$ 23.0	38.6 $\pm$ 1.2	18.3	0.14 $\pm$ 0.03
694-708	EJ200, Texas, US	ESR	55.0 $\times$ 55.0	19.7 $\pm$ 0.6	12.5	0.40 $\pm$ 0.04
Injection Moulded tiles, 3 mm thick						
759	SC301, Protvino, RU	ESR	30.0 $\times$ 30.0	23.4 $\pm$ 0.7	13.9	0.46 $\pm$ 0.07
756-757	SC307, Protvino, RU	ESR	30.0 $\times$ 30.0	23.7 $\pm$ 0.7	14.0	0.12 $\pm$ 0.03
686-7	IMn19, NIU, US	ESR	34.0 $\times$ 34.0	19.3 $\pm$ 0.6	12.4	0.56 $\pm$ 0.08
733-744	IMn21, NIU, US	ESR	36.0 $\times$ 36.0	21.2 $\pm$ 0.6	13.2	0.26 $\pm$ 0.04
726-732	IMn23, NIU, US	ESR	37.0 $\times$ 37.0	17.3 $\pm$ 0.5	11.8	0.04 $\pm$ 0.006
719-725	IMn25, NIU, US	ESR	39.0 $\times$ 39.0	17.7 $\pm$ 0.5	11.2	0.02 $\pm$ 0.003
Calibration Tile, 3.8 mm thick						
662,684-5,746	SCSN-81, Kuraray, JP	Tyvek	30.0 $\times$ 30.0	9.0 $\pm$ 0.3	9.0	1.58 $\pm$ 0.11

Table 2: Beam Test Feb 12-16 2020, 120 GeV protons, FTBF, Hamamatsu SiPM 13360-1350  $1.3 \times 1.3 \text{ mm}^2$ ,  $V_{op} = 54.25 \text{ V}$ .

Runs	Tile Vendor	Wrapping	Area, mm $\times$ mm	MPV, PE	FWHM, PE	Non-Uniformity
Cast tiles, 3 mm thick						
942	EJ208, Texas, US	ESR	30.0 $\times$ 30.0	34.9 $\pm$ 1.0	16.5	0.46 $\pm$ 0.09
931	EJ200, Texas, US	ESR	30.0 $\times$ 30.0	32.8 $\pm$ 1.0	16.8	0.42 $\pm$ 0.08
989	EJ262, Texas, US	ESR	30.0 $\times$ 30.0	34.6 $\pm$ 1.0	16.8	0.33 $\pm$ 0.07
Injection Moulded tiles, 3 mm thick						
988	SC301, Protvino, RU	ESR	30.0 $\times$ 30.0	24.3 $\pm$ 0.7	13.4	0.54 $\pm$ 0.10
996	IMn19, NIU, US	ESR	34.0 $\times$ 34.0	17.4 $\pm$ 0.5	12.4	0.79 $\pm$ 0.12
997	IMn21, NIU, US	ESR	36.0 $\times$ 36.0	16.4 $\pm$ 0.5	11.1	1.19 $\pm$ 0.14
1038,1039	IMn23, NIU, US	ESR	36.0 $\times$ 36.0	17.1 $\pm$ 0.5	11.2	0.49 $\pm$ 0.08
1041	IMn25, NIU, US	ESR	39.0 $\times$ 39.0	17.5 $\pm$ 0.5	11.6	0.65 $\pm$ 0.11
Calibration Tile, 3.8 mm thick						
925,948,949,972,1044	SCSN-81, Kuraray, JP	Tyvek	30.0 $\times$ 30.0	9.5 $\pm$ 0.3	8.8	1.53 $\pm$ 0.18

98 The results are compared to simulation and shown in Fig 3. A  $\chi^2$  fit to data is performed with  
 99 the function  $p_0 \times (\text{Tile Area}/9 \text{ cm}^2)^{p_1}$ , where  $p_0$  and  $p_1$  are parameters of the fit and fitted  
 100 values of  $p_0 = 23.11 \pm 1.43 \text{ PE}$  and  $p_1 = -0.59 \pm 0.17$  are extracted.

## 101 9.1 Test beam vs cosmic light yield

102 To check the validity of comparing light yields measured with the cosmic test stand to light  
 103 yields obtained with test beam data, a few measurements were made with both setups using  
 104 different configurations. These measurements were done with the  $3 \times 3 \times 0.3 \text{ cm}^3$  EJ-200 tile  
 105 wrapped in ESR with holes in the reflector of 3.2 mm and 6.35 mm diameter. The tile was placed  
 106 on an S14160 SiPM operated at  $V_{op}=41.83 \text{ V}$  and sitting on white silk screened backplate or the

Table 3: Beam Test Feb 12-16 2020, 120 GeV protons, FTBF, Hamamatsu SiPM 14160-1315  $1.3 \times 1.3 \text{ mm}^2$ ,  $V_{op} = 41.83 \text{ V}$ .

Runs	Tile Vendor	Wrapping	Area, mm $\times$ mm	MPV, PE	FWHM, PE	Non-Uniformity
Cast tiles, 3 mm thick						
1084	EJ208, Texas, US	ESR	30.0 $\times$ 30.0	30.2 $\pm$ 0.9	17.6	0.42 $\pm$ 0.08
1052	EJ200, Texas, US	ESR	30.0 $\times$ 30.0	30.9 $\pm$ 0.9	17.7	0.65 $\pm$ 0.11
1075	EJ262, Texas, US	ESR	30.0 $\times$ 30.0	28.9 $\pm$ 0.9	17.0	0.53 $\pm$ 0.09
Injection Moulded tiles, 3 mm thick						
1074	SC301, Protvino, RU	ESR	30.0 $\times$ 30.0	21.3 $\pm$ 0.6	13.4	0.56 $\pm$ 0.10
Calibration Tile, 3.8 mm thick						
1051	SCSN-81, Kuraray, JP	Tyvek	30.0 $\times$ 30.0	7.4 $\pm$ 0.2	7.8	1.77 $\pm$ 0.15

107 white backplate covered with black tape. The results from the two test stands gave reasonable  
108 agreement as can be seen in Table 4.

Table 4: Comparison of cosmic test stand and test beam data using the  $3 \times 3 \times 0.3 \text{ cm}^3$  EJ-200 tile wrapped in ESR and the SiPM 14160-1315  $1.3 \times 1.3 \text{ mm}^2$ ,  $V_{op} = 41.83 \text{ V}$ .

Test stand	3.2 mm hole, WSS, MPV (PE)	3.2 mm hole, black tape, MPV (PE)	6.4 mm hole, black tape, MPV (PE)
Test beam	36.26 $\pm$ 1.09	35.99 $\pm$ 1.08	27.62 $\pm$ 0.83
Cosmic	36.78 $\pm$ 1.10	35.71 $\pm$ 1.07	26.60 $\pm$ 0.80

## 109 9.2 Light yield as a function of dimple surface

110 Two injection-molded 3x3cm tiles (from NIU) were studied. The molded tiles had very smooth  
111 dimple surfaces. One tile dimple was abraded with sandpaper to make a very matte surface.  
112 The two tiles were measured in the cosmic setup. They were found to have roughly the same  
113 MPV, with the MPV of the nominal tile at  $13.75 \pm 0.41 \text{ PE}$  and for the scratched surface tile at  
114  $14.24 \pm 0.43 \text{ PE}$ . The conclusion is that the surface quality of the dimple has little effect on light  
115 yield.

## 116 9.3 Light yield as a function of SiPM depth

117 The light yield was measured for different SiPM depths into the dimple. This was done by  
118 varying the depth of the S13360 SiPM into the dimple of a  $3 \times 3 \text{ cm}^2$  EJ-200 tile. The SiPM had  
119 no back plane. The cosmic test stand allowed for the relative change in depth to be known  
120 with an accuracy of 0.03 mm. The measurements were done for two different wrapper hole  
121 sizes and the results can be seen in Fig 4. The reduction in light yield as the SiPM goes deeper  
122 into the dimple is caused by light absorption by the SiPM package. And the reduction as the  
123 SiPM is retracted is due to solid angle effects.

## 124 9.4 Light yield as a function of hole size in ESR reflective wrapper

125 The light yield as a function of hole size in the ESR reflector was measured for a  $3 \times 3 \text{ cm}^2$   
126 EJ200 tile wrapped in ESR. One expects that as the hole diameter in the reflective foil decreases,  
127 the light yield should increase, since fewer photons escape through the gap between SiPM and  
128 wrapper. Likewise, it is expected that if the white silkscreen is changed to a non-reflective  
129 surface, the light yield should decrease, since fewer photons reflect back into the tile through  
130 the gap. The light yield was studied for cases of a white silk screened backplate, and holes in  
131 the reflector of 3.2 mm, 5.1 mm, and 6.35 mm diameter. For these hole sizes, the white backplate

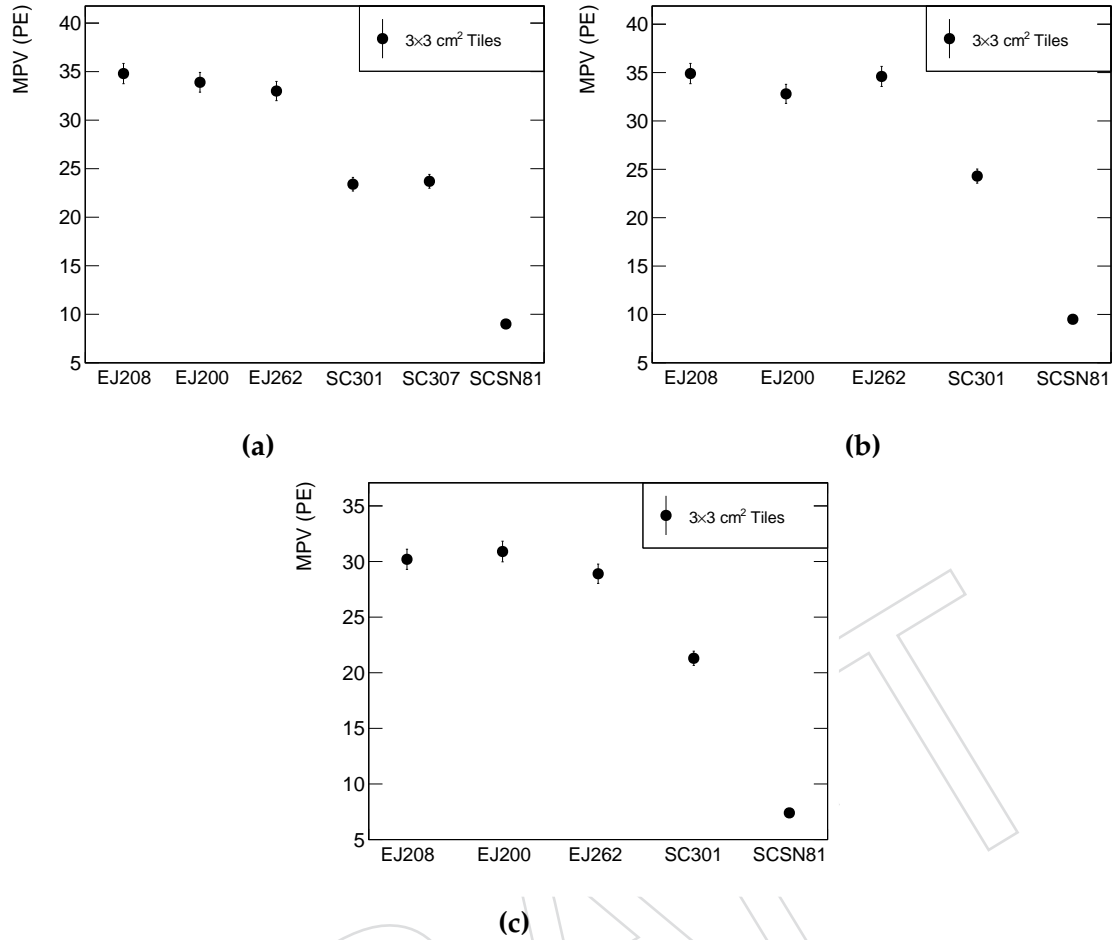


Figure 2: The MPV in  $3 \times 3 \text{ cm}^2$  tiles for a variety of scintillating materials for a) the Hamamatsu SiPM 13360-1350,  $1.3 \times 1.3 \text{ mm}^2$ ,  $V_{op}=54.5 \text{ V}$ , b) the Hamamatsu SiPM 13360-1350  $1.3 \times 1.3 \text{ mm}^2$ ,  $V_{op}=54.25 \text{ V}$ , c) and the Hamamatsu SiPM 14160-1315  $1.3 \times 1.3 \text{ mm}^2$ ,  $V_{op}=41.83 \text{ V}$ .

132 was compared to data taken with the white backplate covered with black tape, which is a good  
 133 approximation to a nonreflective surface. Measurements were also made using the cosmic test  
 134 stand with black tape covering the WSS. The results are compared to simulation and shown in  
 135 Fig. 5. In accordance with our expectations, larger holes had lower light yields, and the effect  
 136 is stronger for the black backplate.

## 137 10 Summary

138 A setup to study the responses of different scintillator tile geometries and materials has been  
 139 installed at the Fermilab Test Beam Facility. The light yield and uniformity was measured for  
 140 various values of the tile size, tile scintillator material, SiPM depth into the tile dimple, and  
 141 the hole diameter in the wrapper. A cosmic test stand was created to verify a subset of these  
 142 measurements. Simulation was developed that agrees well with the light yield and uniformity  
 143 measured in test beam data across the different tiles.

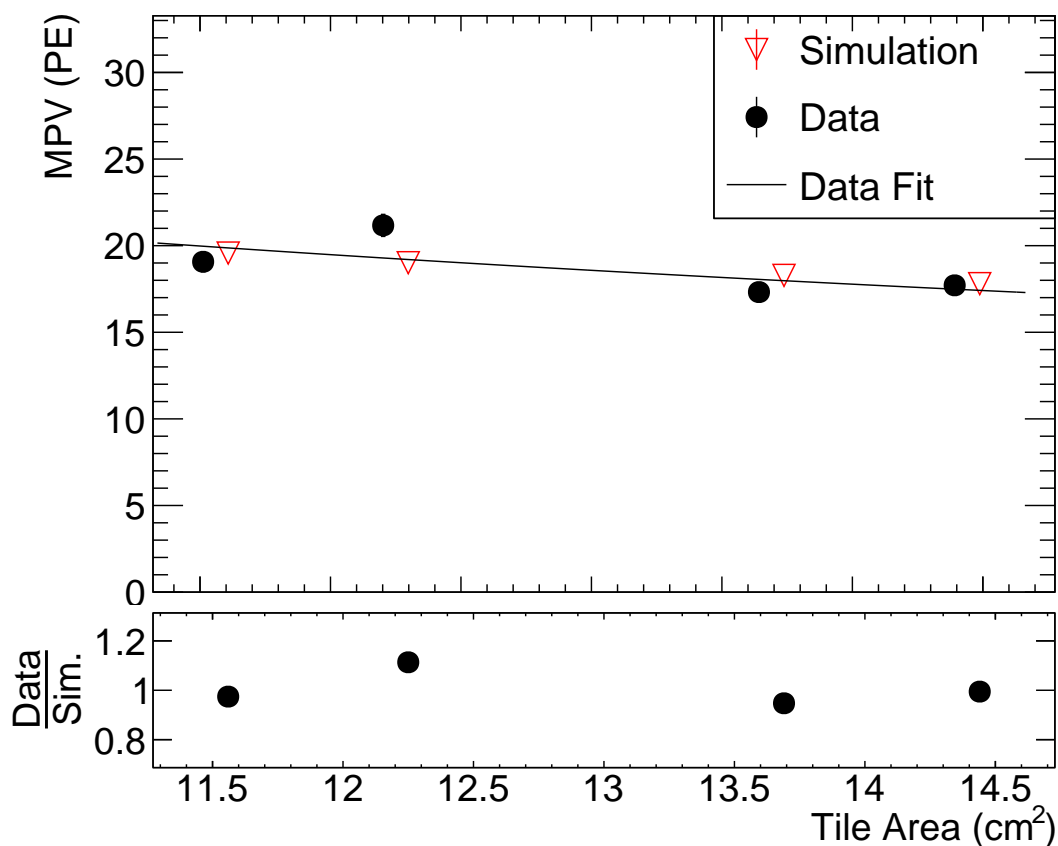


Figure 3: The light yield reported as MPV in data and simulation as a function of tile area for a 3 mm thick, wrapped in ESR, NIU injection moulded scintillator tile. A systematic uncertainty due to reproducibility of optical coupling is estimated to be 3.0%, and is plotted but smaller than the data points. The black curve is the fit to data.

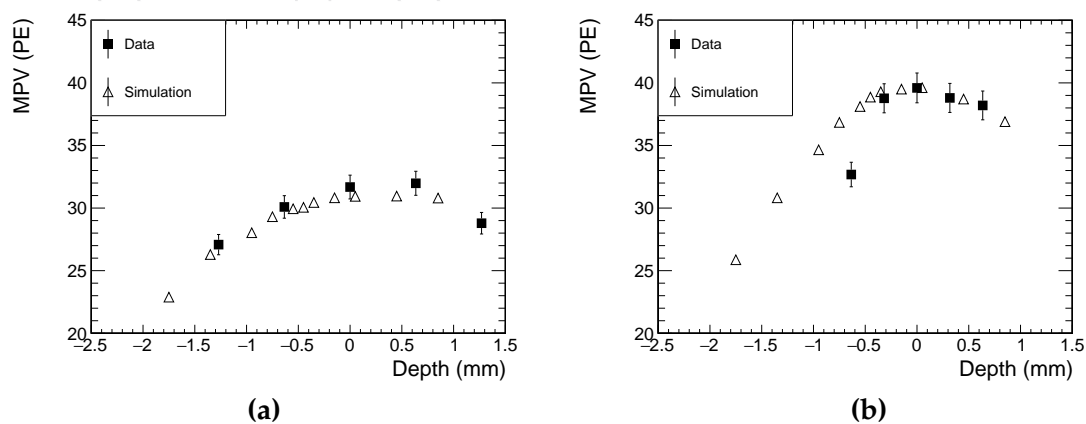


Figure 4: The light yield reported as MPV in data and simulation as a function of SiPM depth into the dimple for a  $3 \times 3$  cm<sup>2</sup> EJ-200 tile with a) 6.4 mm diameter hole and b) the 3.2 mm diameter hole. A negative displacement corresponds to backing the SiPM out of the dimple.

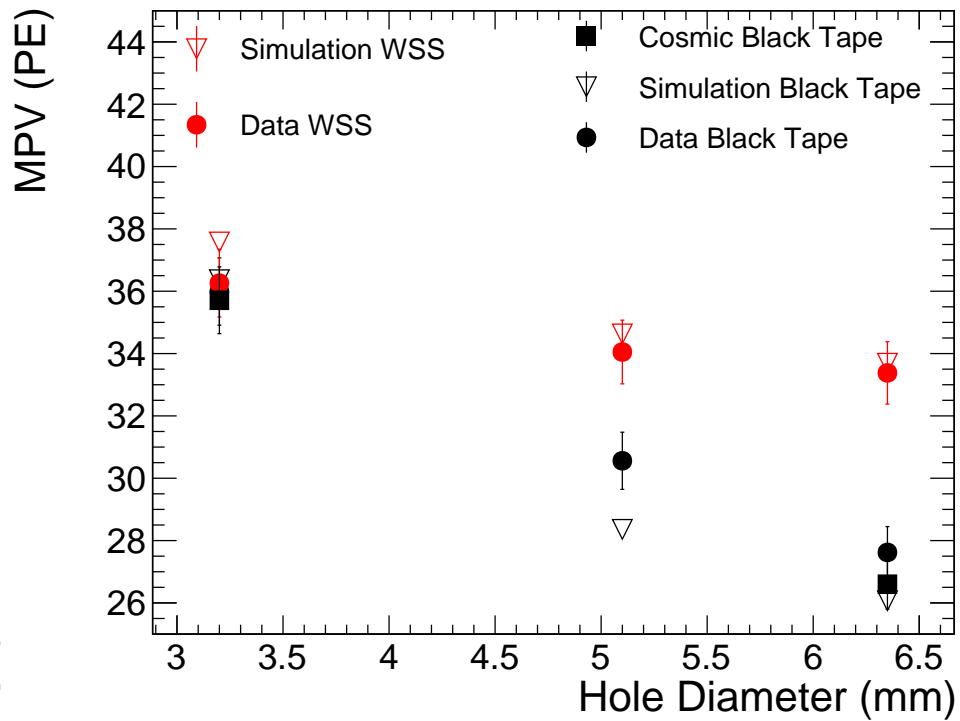


Figure 5: The MPV of the light yields in data (test beam and cosmic test stand) and simulation as a function of hole size are shown for SiPMs sitting on top of a white silkscreened backplate and a black tape backplate. (S13360 SiPM, EJ-200 tile.)



---

## 144 **Acknowledgments**

145 Work supported by the Fermi National Accelerator Laboratory, managed and operated by  
146 Fermi Research Alliance, LLC under Contract No. DE-AC02-07CH11359 with the U.S. De-  
147 partment of Energy. The U.S. Government retains and the publisher, by accepting the article  
148 for publication, acknowledges that the U.S. Government retains a non-exclusive, paid-up, irre-  
149 vocable, world-wide license to publish or reproduce the published form of this manuscript, or  
150 allow others to do so, for U.S. Government purposes. Work also supported by the US-DOE Of-  
151 fice of Science (High Energy Physics) under Award Number DE-SC0011845 and DE-SC0010072.  
152 Additional support provided by the University of Maryland Physics Department.

DRAFT

## References

- 153 [1] A. G. et al., “High-Luminosity Large Hadron Collider (HL-LHC): Technical Design Report  
154 V. 0.1”, Technical Report CERN-2017-007-M, 2017.  
155 doi:doi:10.23731/CYRM-2017-004.  
156
- 157 [2] CMS Collaboration, “The Phase-2 Upgrade of the CMS Endcap Calorimeter”, Technical  
158 Report CERN-LHC-2017-023, 2019.
- 159 [3] G. B. et al., “Directly Coupled Tiles as Elements of a Scintillator Calorimeter with MPPC  
160 Readout”, *Nucl. Instrum. Meth. A* **605** (2009)  
161 doi:doi:10.1016/j.nima.2009.03.253.
- 162 [4] N. Tsuji, “Study on Larger Scintillator Tile for AHCAL”, 2017.
- 163 [5] Y. L. et al., “A Design of Scintillator Tiles Read Out by Surface-Mounted SiPMs for a  
164 Future Hadron Calorimeter”, in *Proceedings, 21st Symposium on Room-Temperature  
165 Semiconductor X-ray and Gamma-ray Detectors*. 2016. arXiv:1512.05900.  
166 doi:doi:10.1109/NSSMIC.2014.7431118.
- 167 [6] E. Niner, “Fermilab Test Beam Facility Status and Plans”, 2020.
- 168 [7] A. Belloni et al., “Test beam study of sipm-on-tile configurations”, 2021.
- 169 [8] GEANT4 Collaboration, “GEANT4—a simulation toolkit”, *Nucl. Instrum. Meth. A* **506**  
170 (2003) 250, doi:10.1016/S0168-9002(03)01368-8.